NONLINEAR ROTOR-FUSELAGE COUPLED RESPONSE TO GENERIC PERIODIC CONTROL MODES USING ADVANCED COMPUTATION TECHNIQUES

S.M. Barkai* and O. Rand**
Faculty of Aerospace Engineering
Technion - Israel Institute of Technology
Haifa 32000, Israel.

ABSTRACT

The paper presents a theoretical study of the interactive periodic vibratory response of a helicopter rotor/fuselage system. The rotor blades and the fuselage are assumed to be fully elastic and the periodic cyclic pitch controls are generic and may contain any number of harmonics. Emphasis is placed on a complete and consistent formulation of all dynamic contributions. This results in highly nonlinear expressions of high harmonic content which are implemented in an advanced computer code. The paper demonstrates a successful combination of two powerful numerical techniques: The method of "Harmonic Variables" and advanced algorithms for solutions of nonlinear systems. This merger minimizes the required analytical effort while preserving high accuracy solution. The potential of the present model to serve as an efficient analytical tool for advanced control concepts such as the High Harmonic Control (HHC) is well established.

INTRODUCTION

Techniques for vibration suppression in rotary wing systems have been under investigation for many years. The development of new methods has continuously accompanied needs of new design concepts. The key to meaningful analytical estimation of the efficiency of any specific method for vibration level reduction is adequate modeling of the rotor/fuselage system as a whole, and a proper, feasible method of solution. It is well known that the helicopter rotor and its fuselage operate in an extremely complex, unsteady environment which poses different modeling challenges such as structural analysis, dynamic aspects and aerodynamic considerations. In advanced realistic models, one also encounters limitations on the required computational effort which become unacceptable in many cases. In addition, many of the proposed means for vibration reduction of helicopters are based on some types of "additional favorable excitation" to the blade pitch control (see Refs. 1,2). Such periodic excitation, which is in the focus of the present analysis, may either be the same for each blade at a given azimuthal location, or different from blade to blade and it is aimed mainly towards the excitation of additional aerodynamic loads. In both cases, this additional excitation complicates the analysis by introducing additional higher pitch harmonics which, due to the inherent nonlinearities of the system and the strong couplings between the various mechanisms, might induce non-negligible changes in many of the system behavior indicators, compared with those obtained in a conventionally controlled system.

From the actual implementation point of view, one should distinguish between two main categories of ways to introduce controls containing high harmonics to the blades. The first category is the one that may be implemented through a conventional swashplate. In this method, one introduces periodic excitation to the swashplate in the nonrotating frame. This technique has already proved to be feasible, and it may be shown that providing that this excitation of the swashplate is based on a frequency, which is a multiple of N_b/rev. (where N_b is the rotor number of blades), all blades are excited identically. This method is broadly referred to as Higher Harmonic Control (HHC) and is well documented in the literature. Application of this method in flight tests is reported in Refs (3-5). Wind tunnel test results are summarized in Refs. (6-7), while Refs. (8-13) represent few of the analytic simulations.

When a conventional swashplate is excited in a frequency which is not a multiply of the rotor rotation frequency, the blades perform different time histories. It may be shown (see Ref. 14) that for $N_b \leq 3$, a conventional swashplates may be used for introducing any individual time history of pitch command for each blade. Indeed, for $N_b > 3$, employing a conventional swashplate which is excited in frequencies that are not multipliers of the rotor rotation frequency, results in non-identical commands for the blades. However, not any different desired time history for each blade may be achieved.

The second category of high harmonic excitation includes commands which are introduced individually by actuators in the rotating frame. This technique is usually referred to as Individual Blade Control (IBC-see Ref. 15) and may be used for general purposes which include cases where all blades undergo identical excitation and cases where different cyclic pitch time histories are introduced for each blade.

*Graduate Student
**Senior Lecturer

Based on the success of the HHC that has been reported in the literature so far, and since the IBC concept is a direct evaluation of the HHC concept, the objectives of the present study were aimed at the modeling and development of an efficient and high resolution formulation and method of solution for a rotor/fuselage system response subjected to generic time histories of cyclic pitch controls. All control modes in the present analysis are introduced to the blade root in the rotating reference system, and therefore, both HHC and IBC pitch command modes may be handled by the present model. Thus, when the blades undergo identical excitation, a representative blade is traced, while in cases where the time history of the pitch command of each blade is different, each blade is traced separately.

Generally, in a trimmed forward flight, the helicopter fuselage undergoes periodic excitation due to many sources. Even by confining the discussion to the vibration induced by the main rotor, in certain configurations one has to take into account not only the vibrations which are transferred to the fuselage through the hub, but also those vibrations which are induced by the blades passage over the fuselage, or by the main rotor wake interaction with the fuselage. However, the study presented in this paper is restricted to the forces and moments which are transferred to the fuselage through the hub.

From a mathematical point of view, each additional component in the harmonic spectrum of the cyclic pitch time history, may be used for vanishing a component in the harmonic spectrum of the vibratory motion. This component may belong to the acceleration of a point in the system or to the forces and the moments which are transmitted through the hub. For example, in the case of conventional HHC excitation, where six additional components are introduced into the vibration spectrum of the swashplate (two due to N_b/rev. collective translation, two due to N_b/rev. lateral tilting and two due to N_b/rev. longitudinal tilting), six components such as the N_b/rev. hub forces in three orthogonal directions (both sine and cosine components) may be set to zero. Clearly, in such a case, not enough degrees of freedom are left for vanishing also the hub moments components or the $p \cdot N_b$/rev. (p=2,3...) harmonics of the hub loads, and a compromise in the form of optimization of the vibratory response at some pre-selected points of the system is inevitable (see also Ref. 2).

ANALYSIS

As already indicated, the numerical implementation of the present analysis is based on the combination of a recently developed concept of "Harmonic Variables" (see Ref. 16) with a nonlinear solver. For the sake of clarification, the above technique of utilizing "Harmonic Variables" will be reviewed first. Then, the various aspects of the present structural dynamic and aerodynamic modeling will be developed and discussed.

Overview of the Harmonic Variables Approach

A harmonic variable is a real number the value of which is changed periodically with a period of 2π. Harmonic variable, F, may therefore be represented by an infinite array of its Fourier coefficients as:

$$F = F_o + \sum_{p=1}^{\infty} \left[F_{cp} \cos(p\psi) + F_{sp} \sin(p\psi) \right] \qquad (1)$$

Truncating the above infinite sum enables one to define a finite harmonic operator, H_q, using finite arrays of real numbers F_{cp} and F_{sp} of dimension q (i.e. p=1,....q) as:

$$F \cong H_q(F_o, F_{cp}, F_{sp}) \equiv F_o + \sum_{p=1}^{q} \left[F_{cp} \cos(p\psi) + F_{sp} \sin(p\psi) \right] \qquad (2)$$

In principle, the periodicity parameter, ψ, may represent any variable, however, in the context of the present study ψ represents a nondimensional time (i.e. $\psi=2\pi t/T$ where t is the time and T is the period). In what follows, all harmonic variables and their coefficients will be denoted as shown in Eq. (2) (i.e., denoting the harmonics by the subscripts $(\ )_o$, $(\ )_{cp}$ and $(\ )_{sp}$). Clearly any constant real number, r, may be represented as the harmonic variable, R, where $R_o=r$, $R_{cp}=R_{sp}=0$ (p=1,....q). In addition, the basic trigonometric functions $\sin(\psi)$ and $\cos(\psi)$ may be described as the harmonic variables S and C, respectively, where $S_{s1}=C_{c1}=1$ and $S_o=C_o=S_{c1}=C_{s1}=0$, $S_{cp}=S_{sp}=C_{cp}=C_{sp}=0$ (p=2,...q). The mathematical operations between harmonic variables that will be discussed in what follows enables the construction of all other trigonometric functions of ψ using the above definitions of the sine and cosine functions.

It should be noted that there is an interesting analogy between the number of coefficients used to describe a harmonic variable and the number of digits used to describe a real number. This is due to the fact that similar to real numbers, adding and subtracting of harmonic variables do not change the required number of coefficients. However, multiplying two harmonic variables represented by q_1 and q_2 harmonics, respectively, results in a harmonic variable having q_1+q_2 coefficients. Moreover, division of harmonic variables results in an infinite number of additional harmonics.

Basic mathematical operations between harmonic variables are similar to those of real numbers and may be executed by determining the coefficient of the resulting harmonic variable directly by using the coefficients of the involved variables. Additions and subtractions are trivial and are essentially based on adding or subtracting the corresponding harmonics (see Ref. 16). Multiplying two harmonic variables is based on the appropriate trigonometric identities and may be put in the following form for the case of $E=F \cdot G$:

$$\begin{Bmatrix} E_o \\ E_{c1} \\ \vdots \\ E_{cq} \\ E_{s1} \\ \vdots \\ E_{sq} \end{Bmatrix} = [\bar{G}] \begin{Bmatrix} F_o \\ F_{c1} \\ \vdots \\ F_{cq} \\ F_{s1} \\ \vdots \\ F_{sq} \end{Bmatrix} \qquad (3)$$

where $[\bar{G}]$ is a matrix which is a function of the coefficients of the harmonic variable G only, namely: G_o, G_{cp}, G_{sp} (p=1,....q). This matrix is generated symbolically for any given number of harmonics by a separate special purpose computer code. Division of harmonic variables is based on the above multiplication operation. More details may be found in Ref. 16.

Analytic functions of harmonic variables result in harmonic variables as well. Using the above basic mathematical operations, analytic functions are generated by expanding the functions into power series.

Differentiation of harmonic variables with respect to the periodicity parameter, ψ, results in harmonic variables as well - see Ref. 16. It should also be mentioned that all explicit numerical schemes for differentiation and integration that have been developed for real numbers may be directly applied to harmonic variables as well. As an example, numerical differentiation with respect to any variable (other than ψ), say x, may be put in the general form:

$$\left.\frac{\partial^n F}{\partial x^n}\right|_{x=x_0} = \frac{1}{\delta^n}\sum_{k=1}^{K} r(k,n)F(x_0+x_k) \qquad (4)$$

where δ is a typical length, x_k are intervals around x_0 and r(k,n) are weight coefficients associated with the specific finite differences scheme. Clearly, since F is a harmonic variable the resulting derivative is also a harmonic variable. Similarly, numerical integration with respect to x may be performed. Other operations with harmonic variables may be found in Ref. 16.

The implementation of harmonic variables in numerical codes is carried out using a "super compiler" which has been developed along the above guidelines. This is a computer code that converts codes that were written using harmonic variables to standard computer codes. As far as the user is concerned, all operations with harmonic variables, (additions, multiplications, analytic functions etc.) are written in the standard form as if they were real numbers. A simple application is presented in Fig. 1.

Consequently, this technique allows for enormous reduction in the required analytic effort in cases where highly nonlinear terms which have to be expressed with high harmonic resolution are involved. Moreover, since all operations are symbolically coded, increasing the number of harmonics does not cause any changes in the analytic derivation or in the computer code and it is executed automatically by changing the harmonic variables dimension q, (see Eq. 2.).

Systems of Coordinates

The present formulation is based on five systems of coordinates. The systems and their mutual transformations are described in this section. As will be clarified in what follows, each system and quantities in its directions are denoted by one of the indices G, F, H, B and D, while the corresponding axes are denoted by x_G, y_G, z_G etc., and unit vectors in these directions are denoted $\hat{x}_G$, $\hat{y}_G$, $\hat{z}_G$ etc. Any other quantity belonging to a system will be indicated as $(\ )_G$ etc.

```
      c
      c  Declaring HA,HB,HC as Harmonic Variables
      c  of 8 harmonics(i.e. 17 coefficients)
      c  and double precision (*8).
      c
           HARMONIC(17)*8 HA,HB,HC
      c
      c  Setting HA to be:
      c  1.+2.*Sin(Psai)+3.*Cos(2.*Psai)
      c
           HA=SET(0.D0)
           HA=INPUTC(1.D0,0)
           HA=INPUTS(2.D0,1)
           HA=INPUTC(3.D0,2)
      c
      c  Printing HA
      c
           WRITE(10,*)'==========  HA  =========='
           HA=PRINT(HA)
      c
      c  Setting HB to be:
      c  4.+5.*Sin(3.*Psai)+6.*Cos(4.*Psai)
      c
           HB=SET(0.D0)
           HB=INPUTC(4.D0,0)
           HB=INPUTS(5.D0,3)
           HB=INPUTC(6.D0,4)
      c
      c  Printing HB
      c
           WRITE(10,*)'==========  HB  =========='
           HB=PRINT(HB)
      c
      c  Setting HC=HA*HB
      c
           HC=HA*HB
      c
      c  Printing HC
      c
           WRITE(10,*)'==========  HC  =========='
           HC=PRINT(HC)
      c
           STOP
           END
```

a)

```
 ==========  HA  ==========
       0     1.0000          0.00000E+00
       1     0.00000E+00      2.0000
       2     3.0000          0.00000E+00
       3     0.00000E+00     0.00000E+00
       4     0.00000E+00     0.00000E+00
       5     0.00000E+00     0.00000E+00
       6     0.00000E+00     0.00000E+00
       7     0.00000E+00     0.00000E+00
       8     0.00000E+00     0.00000E+00
 ==========  HB  ==========
       0     4.0000          0.00000E+00
       1     0.00000E+00     0.00000E+00
       2     0.00000E+00     0.00000E+00
       3     0.00000E+00      5.0000
       4     6.0000          0.00000E+00
       5     0.00000E+00     0.00000E+00
       6     0.00000E+00     0.00000E+00
       7     0.00000E+00     0.00000E+00
       8     0.00000E+00     0.00000E+00
 ==========  HC  ==========
       0     4.0000          0.00000E+00
       1     0.00000E+00      15.500
       2     26.000          0.00000E+00
       3     0.00000E+00     -1.0000
       4     1.0000          0.00000E+00
       5     0.00000E+00      13.500
       6     9.0000          0.00000E+00
       7     0.00000E+00     0.00000E+00
       8     0.00000E+00     0.00000E+00
```

b)

Fig. 1: An application of "Harmonic variables".

a) The code (includes the input and a multiplication operation).

b) The output.

The G (gravity) system is an inertial reference system while gravity is assumed to act in the $-\hat{z}_G$ direction.

The F (fuselage) system is a system which is attached to the fuselage (see Fig. 2). The transformation of a physical vector from the G system to the F system is executed by the transformation matrix $[T_{FG}]$, namely:

$$\begin{pmatrix} x_F \\ y_F \\ z_F \end{pmatrix} = \left[T_{FG}\right] \begin{pmatrix} x_G \\ y_G \\ z_G \end{pmatrix} \qquad (5)$$

where the $[T_{FG}]$ matrix is a function of the fuselage attitude angles θ_{Fx}, θ_{Fy}, and θ_{Fz}. By setting $\theta_{Fz}=0$, the helicopter fuselage is assumed to be placed in a plane which is parallel to the $\hat{x}_G$-$\hat{z}_G$ plane.

The H (hub) system is attached to the F system at the coordinate $x_F=x_h$, $z_F=z_h$ (see Fig. 2) and is rotating in a constant angular velocity $\Omega\hat{z}_F$. Although this system is excited by the vibratory deformation of the fuselage, the differences between the F and H attitudes are ignored. Similar to Eq. (5), the transformation between the F and the H systems are based on the $[T_{HF}]$ matrix which is a function of the azimuth angle of the reference blade, ψ.

The B (blade) system is connected to the H system at $e\hat{x}_H$ and its attitude is determined by the three root angles β, ζ, θ. β is the flapping angle, ζ is the lead-lag angle and θ is the pitch angle. The transformation matrix between the H and B the systems is denoted $[T_{BH}]$.

The D (deformed) system is a local system of coordinates which is attached to each cross-section along the blade. The attitude of this system is determined by the local elastic deformation values which will be dealt with in what follows within the description of the structural modeling. The transformation matrix between the B and the D systems is denoted $[T_{DB}]$. Before deformation the blade elastic axis is assumed to be straight and to coincide with the x_B axis. Thus, the blade cross-sections may be identified by their spanwise location $x(\equiv x_B)$. While the elastic elongation of the blade is neglected, the present analysis accounts for the shortening of the distance of each cross-section to the rotating axis induced by the transverse displacements v, w - see Fig. 3. Thus, the location of the D system root is at $x_B=x+s$, $y_B=v$, $z_B=w$, where:

$$s(x) \cong -\frac{1}{2}\int_0^x (w_{,x}^2 + v_{,x}^2)\,dx' \qquad (6)$$

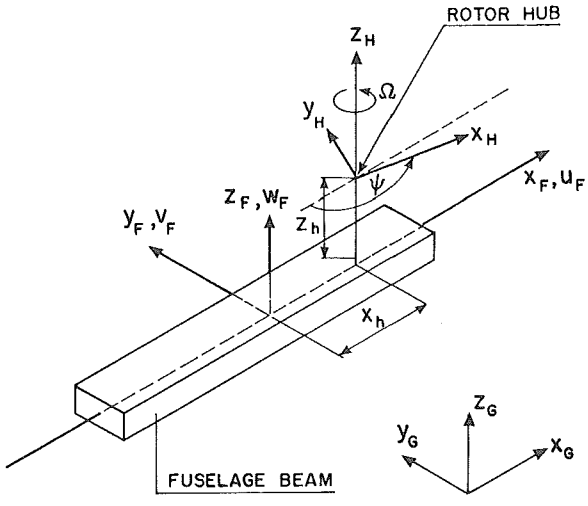

Fig. 2: The Gravity, Fuselage and Hub systems of coordinates.

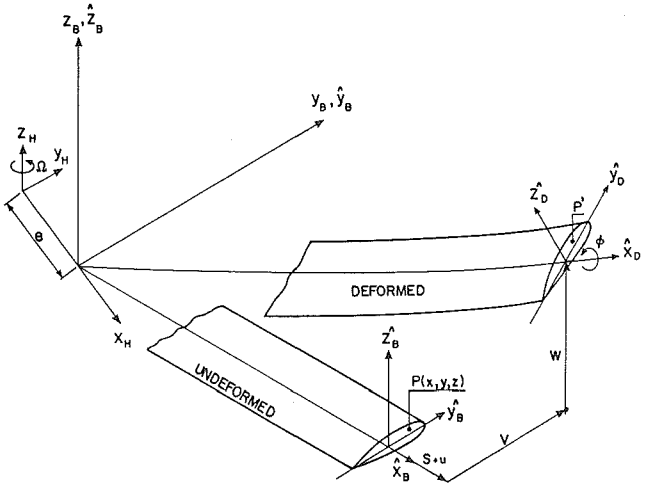

Fig. 3: The Hub, Blade and Deformed systems of coordinates.

The Structural Modeling

The elastic blades: The structural analysis used in the present modeling for determining the periodic elastic motion of the blades is based on the generic nonlinear beam model described in Ref. 17. The nonlinear terms in this model are derived for small strains and moderate elastic rotations. The above generic analysis has been reduced to the present case where the undeformed blades are assumed to be straight and untwisted while their elastic axis coincides before deformation with the $\hat{x}_H$ coordinate line (see Figs. 2,3). Deformation is assumed to consist of the displacements u, v, and w in the $\hat{x}_B$, $\hat{y}_B$ and $\hat{z}_B$ directions, respectively. In addition, a twist angle, ϕ, is assumed to occur about the elastic axis in its position after the displacements u, v and w took place. As shown in Ref. 17, the bending moments components in this case are given by:

$$M_x = (GJ + \frac{PI_p}{A})T \qquad (7a)$$

$$M_y = -EI_{yz}K_y - EI_{zz}K_z + Pz_c \qquad (7b)$$

$$M_z = EI_{yy}K_y + EI_{yz}K_z - Py_c \qquad (7c)$$

P is the tensile force and y_c, z_c are the cross-sectional coordinates of the center of tension. K_y, K_z and T are the curvatures in $\hat{y}_D$ and z_D directions, and the twist, respectively. These curvatures are given by:

$$T = \phi_{,x} + (v_{,xx} + w_{,xx}\phi)(w_{,x} - v_{,x}\phi) \qquad (8a)$$

$$K_y = v_{,xx} + w_{,xx}\phi \qquad (8b)$$

$$K_z = w_{,xx} - v_{,xx}(\phi + v_{,x}w_{,x}) \qquad (8c)$$

where $(\ )_{,x}$ stands for differentiation with respect to the blade length. The six equilibrium equations for forces and moments acting on each segment of the beam are also presented in Ref. 17. Elimination of the shear resultant forces from these equations yields the following four differential equations of equilibrium:

$$P_{,x} = -p_x + K_yV_y + K_zV_z \qquad (9a)$$

$$K_yP - (EI_{yy}v_{,xx} + EI_{yz}w_{,xx})_{,xx} = -p_y + TV_z + q_{ze,x} \qquad (9b)$$

$$K_zP - (EI_{yz}v_{,xx} + EI_{zz}w_{,xx})_{,xx} = -p_z - TV_y - q_{ye,x} \qquad (9c)$$

$$(GJ\phi_{,x})_{,x} = -q_x + K_yM_y + K_zM_z \qquad (9d)$$

where q_{ze}, q_{ye} are equivalent load components which are given by:

$$q_{ze} = q_z + [EI_{yy}w_{,xx}\phi - EI_{yz}v_{,xx}(\phi + v_{,x}w_{,x}) - Py_c]_{,x} + K_zM_x + TM_y \qquad (10a)$$

$$q_{ye} = q_y + [-EI_{yz}w_{,xx}\phi - EI_{zz}v_{,xx}(\phi + v_{,x}w_{,x}) + Pz_c]_{,x} + K_yM_x - TM_z \qquad (10b)$$

and V_y, V_z are the cross-sectional forces resultants:

$$V_y = -[EI_{yy}v_{,xx} + EI_{yz}w_{,xx}]_{,x} - q_{ze} \qquad (11a)$$

$$V_z = -[EI_{yz}v_{,xx} + EI_{zz}w_{,xx}]_{,x} + q_{ye} \qquad (11b)$$

The associated nonlinear form of the boundary conditions are given in Ref. 17, and similar to the solution procedure described there, Eqs. 9a-d, are solved by Galerkin method where the shape functions are the natural mode shapes.

The elastic fuselage: From a structural point of view the fuselage is treated as a beam and the structural modeling is based on modal analysis. The fuselage and its system of coordinates x_F, y_F and z_F are presented schematically in Fig. 2. The fuselage structural behavior is assumed to be characterized by small linear deflection in which lateral and torsion elastic motions are uncoupled. Thus, the elastic lateral deflections and the elastic torsion are given by:

$$w_F(x_F) = \sum_{i=1}^{N_{W_F}} \xi_w^i(t) \cdot \Phi_w^i(x_F) \qquad (12a)$$

$$v_F(x_F) = \sum_{i=1}^{N_{V_F}} \xi_v^i(t) \cdot \Phi_v^i(x_F) \qquad (12b)$$

$$\phi_F(x_F) = \sum_{i=1}^{N_{\phi_F}} \xi_\phi^i(t) \cdot \Phi_\phi^i(x_F) \qquad (12c)$$

As a beam, the fuselage boundary conditions are "free" at both ends. To account for rigid motions, the first modes have been chosen as follows:

$$\Phi_w^1 = \Phi_v^1 = \Phi_\phi^1 = 1 \qquad (13a)$$

$$\Phi_w^2 = \Phi_v^2 = \frac{x_F - x_{FCG}}{L_F} \qquad (13b)$$

where x_{FCG} and L_F are the fuselage center of gravity coordinate and its length, respectively, and the successive modes were the corresponding elastic modes. Since uncoupled elastic behavior is assumed, the following discussion will be concentrated in the vertical motion, w_F, while the formulation of the lateral motion v_F and the elastic motion Φ_F are similar. Since Φ_w^i are orthogonal modes, the governing equation for the ith mode becomes:

$$M_w^i\ddot{\xi}_w^i\Omega^2 + M_w^iC_w^i\dot{\xi}_w^i\Omega + M_w^i\omega_w^{i\,2}\xi_w^i = F_w(\psi)\Phi_w^i(x_h) - Q_w(\psi)\frac{\partial\Phi_w^i}{\partial x_F}(x_h) \qquad (14a)$$

where:

$$M_w^i = \int_0^{L_F} \phi_w^{i\,2}(x_F')m(x_F')dx_F' \qquad (14b)$$

C_w^i is a generalized damping coefficient, ω_w^i is the ith mode frequency, m is the fuselage mass per unit length and $F_w(\psi)$ and $Q_w(\psi)$ are the concentrated force and moment, respectively, that acts at the hub ($x_F=x_h$) due to the main rotor. $(\dot{})$ stands for differentiation with respect to the azimuth angle, ψ. Within the present study, it is assumed that all loads acting over the fuselage, except the hub loads are of low frequency and will be considered as constant in what follows. Assuming identical time history for all blades, the hub load which is transferred to the fuselage, F_w and Q_w, contains only harmonics which are multipliers of the rotor number of blades and may therefore be expressed as harmonic variables containing non-vanishing values only for the pth harmonic where $p=N_b, 2N_b \ldots$. Consequently, each of the modes coefficients ξ_w^i may also be expressed as harmonic variables, and Eq. (14a) implies that for $p=N_b, 2N_b \ldots$:

$$\begin{Bmatrix} \xi^i_{wcp} \\ \xi^i_{wsp} \end{Bmatrix} = \frac{1}{A^{i\,2}_w + B^{i\,2}_w} \cdot$$

$$\cdot \begin{bmatrix} A^i_w & -B^i_w \\ B^i_w & A^i_w \end{bmatrix} \begin{Bmatrix} \phi^i_w(x_h)F_{wcp} - \dfrac{\partial \phi^i_w}{\partial x_F}(x_h)Q_{wcp} \\ \phi^i_w(x_h)F_{wsp} - \dfrac{\partial \phi^i_w}{\partial x_F}(x_h)Q_{wsp} \end{Bmatrix} \quad (15)$$

where:

$$A^i_w = M^i_w\left(\omega^{i\,2}_w - p^2\Omega^2\right) \quad (16a)$$

$$B^i_w = M^i_w C^i_w p\Omega \quad (16b)$$

and for any p which is not a multiple of N_b, $\xi^i_{wcp}=\xi^i_{wsp}=0$. As for the constant values ξ^i_{wo}, it is possible to show that for the rigid modes, these values vanish due to trim considerations, while the constant values of the other (elastic) modes do not necessarily vanish and they are determined by the assumed steady load distribution over the fuselage and are not of interest in the present context. Based on Eq. (12a), the acceleration in the w_F direction at a given point $x_F=x_p$ along the fuselage is given by:

$$\overset{**}{w}_F(x_p) = \sum_{p=N_b,2N_b\ldots} G(p,x_p)\cos(p\psi - \beta(p)) \quad (17)$$

where according to the present analysis

$$G(p,x_p) = -\sum_{i=1}^{N_{w_F}} p^2\sqrt{\xi^{i\,2}_{wcp}+\xi^{i\,2}_{wsp}}\;\Phi^i_w(x_p) \quad (18)$$

Alternatively, both $G(p,x_p)$ and $\beta(p)$ may be extracted experimentally from standard vibration testing of the isolated fuselage (e.g., Ref. 18). In such testing, the fuselage is excited in various frequencies by a periodic force at the hub and the acceleration absolute value, $G(p,x_p)$ and the phase angle $\beta(p)$ at some prescribed locations over the fuselage are directly measured. Clearly, for determining the rotor/fuselage coupled response, $G(p,x_h)$ and $\beta(p)$ ($p=N_b,2N_b\ldots$) are sufficient. Then, to determine the vibration level at x_p, $G(p,x_h)$ is also required.

Longitudinally, the fuselage is assumed to be stiff. Thus, by choosing one mode in this direction, and a shape function $\Phi_u=1$, the longitudinal rigid body vibratory motion may be determined along the same lines described above for the other directions.

The Inertial Loads

To find the inertial loads at a certain cross-section in the local D system coordinates directions, one has to express the inertial acceleration of each material point over the cross-section under discussion. For the sake of convenience, two position vectors, $\bar{R}_H$ and $\bar{R}_M$ are defined. The vector $\bar{R}_H$ connects the G (inertial) system origin, with the H system origin while the (rotating) vector $\bar{R}_M$ connects the H system origin with a generic material point, P, which has been located before deformation at $x_B=x$, $y_B=y$, $z_B=z$ (see Fig. 3). Based on the above described system of coordinates, $\bar{R}_H$ and $\bar{R}_M$ are given by:

$$\bar{R}_H = \begin{Bmatrix} Ut \\ Vt \\ Wt \end{Bmatrix}_G + \begin{Bmatrix} x_h + u_F - z_h w_{F,x} - z_h v_{F,x} \\ v_F - z_h\theta_{Fx} \\ w_F + z_h \end{Bmatrix}_F \quad (19)$$

$$\bar{R}_M = \begin{Bmatrix} e \\ 0 \\ 0 \end{Bmatrix}_H + \begin{Bmatrix} x+s \\ v \\ w \end{Bmatrix}_B + \begin{Bmatrix} 0 \\ y \\ z \end{Bmatrix}_D \quad (20)$$

where U, V and W are the helicopter velocity components in the $\hat{x}_G, \hat{y}_G, \hat{z}_G$, directions, respectively.

By denoting $(\overset{*}{})$ and $(\overset{\circ}{})$ as the nondimensional derivatives (i.e. the dimensional derivative divided by Ω) relative to the G and the H systems, respectively, the inertial nondimensional acceleration of the above generic material point is given by:

$$\bar{a}_G = \overset{**}{\bar{R}_H} + \overset{*}{\bar{\Omega}} \times \bar{R}_M + \bar{\Omega} \times (\bar{\Omega} \times \bar{R}_M) + 2\bar{\Omega} \times \overset{\circ}{\bar{R}} + \overset{\circ\circ}{\bar{R}_M} \quad (21)$$

Since the rotor angular speed is constant and the rates of the attitude change of the H system due to the elastic motion of the fuselage are neglected, $\bar{\Omega}$ may be expressed as:

$$\bar{\Omega} = \begin{Bmatrix} 0 \\ 0 \\ \Omega \end{Bmatrix}_H \quad (22)$$

Assuming steady flight where U, V and W are constants, $\bar{a}_G$ may be expressed as:

$$\bar{a}_G = \begin{Bmatrix} a_x + a_{xy}y + a_{xz}z \\ a_y + a_{yy}y + a_{yz}z \\ a_z + a_{zy}y + a_{zz}z \end{Bmatrix}_D \quad (23)$$

Integrating the above acceleration results in the distributed forces and moments due to the inertia. These loads are given by:

$$\bar{p}_a = -\iint_A \bar{a}_G\,\rho\,dA \quad (24)$$

$$\bar{q}_a = -\iint_A (y\hat{x}_D - z\hat{z}_D) \times \bar{a}_G\,\rho\,dA \quad (25)$$

where ρ is the material density. These expressions may be explicitly expressed as:

$$p_\alpha = -m(a_\alpha + y_{cg}a_{\alpha y} + z_{cg}a_{\alpha z}) \quad ; \quad (\alpha = x,y,z) \quad (26)$$

$$q_x = - m(y_{cg}a_z - z_{cg}a_y + I_{yy}a_{zy} - I_{zz}a_{yz} + I_{yz}(a_{zz} - a_{yy}) \quad (27a)$$

$$q_y = - m(z_{cg}a_x + I_{yz}a_{xy} + I_{zz}a_{xz}) \quad (27b)$$

$$q_z = - m(-y_{cg}a_x - I_{yz}a_{xz} - I_{yy}a_{xy}) \quad (27c)$$

where:

$$(m,\ my_{cg},\ mz_{cg},\ mI_{yy},\ mI_{yz},\ mI_{zz}) = \iint_A \rho(1, y, z, y^2, yz, z^2)\ dA \quad (28)$$

The Aerodynamic Loads

The dynamic velocity: To determine the aerodynamic loads which are distributed along the blade, one first has to evaluate the components of the dynamic velocity at each cross-section. Since the present analysis deals with motions containing high harmonics, exact and complete expressions for the dynamic velocity which are fully consistent with the dynamic response of both rigid and elastic degrees of freedom of the systems, are required.

Based on the previously defined $\bar{R}_H$ and $\bar{R}_M$ vectors, the velocity of each material point is given by:

$$\bar{v}_G = \overset{*}{\bar{R}}_H + \bar{\Omega} \times \bar{R}_M + \overset{\circ}{\bar{R}}_M \quad (29)$$

Similar to Eq. (23), $\bar{v}$ may be expressed as:

$$\bar{v}_G = \begin{Bmatrix} v_x + v_{xy}y + v_{xz}z \\ v_y + v_{yy}y + v_{yz}z \\ v_z + v_{zy}y + v_{zz}z \end{Bmatrix}_D \quad (30)$$

The distributed loads: The following expressions for the aerodynamic loads are based on a two-dimensional unsteady strip theory and the classical Theodorsen theory and its extension for periodic free stream velocity proposed by Greenberg (see Ref. 19). Employing such a two-dimensional unsteady strip theory combined with a prescribed inflow model is based on separating the flow-field into "inner" and "outer" regions. In the "inner" two-dimensional flow-field, the loads are calculated by taking into account inflow induced by the trailing vortices and the magnitude and phase shift variations induced by the "near" shed wake vortices. In the "outer" flow-field, the trailing vortices induced velocity is determined. The prescribed inflow model used in the present model as the trailing vortices induced velocity is assumed to be steady at a given location over the disk. This assumption is justified since the present modeling is concentrated in a steady trimmed flight where the changes in the overall thrust and moments acting on the fuselage are negligible. On the other hand, the local variations of loads are rapid in the case of pitch commands of high harmonics content, and unsteady treatment of the "inner" flow-field which yields loads distribution is inevitable.

Figure 4 presents the y_D-z_D plane of the local deformed system of coordinates where the airfoil is represented as a thin flat chord in accordance with

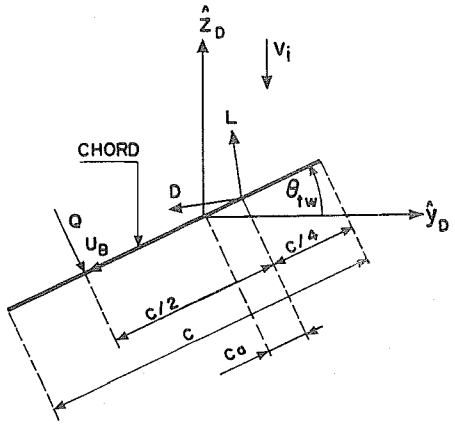

Fig. 4: Notation for the cross-sectional aerodynamic analysis.

the above mentioned Greenberg's theory used in this formulation. Since the loads depend on the free stream velocity, U_B, and the three-quarter normal velocity, Q, these quantities will be determined first. In the present analysis U_B and Q should be evaluated at the three-quarter chord location the coordinates of which in the $\hat{y}_D$-$\hat{z}_D$ directions are given by (see Fig. 4):

$$y_{TQ} = - C\left(\frac{1}{2} - a\right)\cos\theta_{tw} \quad (31a)$$

$$z_{TQ} = - C\left(\frac{1}{2} - a\right)\sin\theta_{tw} \quad (31b)$$

where C and θ_{tw} are the blade chord and the twist angle, respectively, and Ca is the distance between the forward quarter-chord and the $\hat{y}_D$-$\hat{z}_D$ origin (see Fig. 4). Substituting the above coordinates in the velocity expressions of Eq. (30), yields the velocity v_y and v_z in the $\hat{y}_D$ and $\hat{z}_D$ directions, respectively. By geometrical consideration it is clear that Q and U_B are then given by (see Fig. 4):

$$Q = -v_y\sin\theta_{tw} + (v_z + v_i)\cos\theta_{tw} \quad (32)$$

$$U_B = v_y\cos\theta_{tw} + (v_z + v_i)\sin\theta_{tw} \quad (33)$$

v_i is the external inflow velocity (which is assumed to be in the $-\hat{z}_D$ direction and constant over the cross-section) and similar to v_y, v_z, Q and U_B, is a function of both the spanwise and the azimuthal location over the disk.

Having Q and U_B in hand, the circulatory lift may be expressed as:

$$L = - 2\pi\rho_a U_B b\ C(k)\ Q \quad (34)$$

where ρ_a is the air density and b is the semi-chord. C(k) is the Theodorsen lift deficiency (complex) function. Note that C(k) should be a function

of the reduced frequency $k=\omega b/U_B$. As in Greenberg's theory, U_B in the case of oscillating free stream velocity is replaced by its constant (mean) value, U_{Bo}. Thus, the reduced frequency of the p^{th} harmonic becomes:

$$k_p = \frac{p\Omega b}{U_{Bo}} \tag{35}$$

Rational approximation for $C(k_p)$ and its usage in Eq. (34) appears in Ref. 20. Drag is approximated as a quasi-steady force which depends on the instantaneous free stream velocity. Since lift and drag act perpendicular to and in the direction of the resultant velocity, respectively, the aerodynamic loads due to the lift, p_y^A and p_z^A in the $\hat{y}_D$ and $\hat{z}_D$ directions, respectively, may be expressed as (see Fig. 4):

$$p_y^A = \rho_a b\left[2\pi(v_z + v_i)C(k)Q - v_y U_B C_d\right] \tag{36a}$$

$$p_z^A = -\rho_a b\left[2\pi v_y C(k)Q + (v_z + v_i)U_B C_d\right] \tag{36b}$$

Again, it should be emphasized that v_z, v_i, Q and v_y are all periodic. In addition, the blade undergoes an aerodynamic moment due to the above lift which is given by:

$$q_x^A = Ca\left(p_z^A\cos\theta_{tw} - p_y^A\sin\theta_{tw}\right) \tag{36c}$$

while the aerodynamic moment due to the profile camber and the moment associated with the drag are neglected.

As already indicated, the inflow at each cross-section is assumed to be an harmonic variable, and therefore, any prescribed values of inflow may be introduced. The results presented in this paper are based on the classical inflow variation which includes one harmonic having coefficients that vary linearly along the blade span, namely:

$$v_{io} = \bar{v}_i \tag{37a}$$

$$v_{ic1} = \bar{v}_i k_c\, x/L \tag{37b}$$

$$v_{is1} = \bar{v}_i k_s\, x/L \tag{37c}$$

$$v_{icp} = v_{isp} = 0 \quad (p \geq 2) \tag{37d}$$

where $\bar{v}_i$ is Glauert's averaged (momentum-based) induced velocity over the disk.

Hub Loads

Hub loads are obtained by direct integration of the distributed loads along the blade. For that purpose, all distributed loads and moments originally developed in the D system are first transformed to the B system. Then all quantities are integrated which may be expressed as:

$$[F_{xB},\ F_{yB},\ F_{zB}] = \int_0^L [p_{xB},\ p_{yB},\ p_{zB}]dx \tag{38a}$$

$$[M_{xB},\ M_{yB},\ M_{zB}] =$$

$$= \int_0^L [q_{xB} + vp_{zB} - wp_{yB},\ q_{yB} + wp_{xB} - (x+s)p_{zB},$$

$$q_{zB} + (x+s)p_{yB} - vp_{xB}]dx \tag{38b}$$

Thus, the hub forces and moments in the rotating H system are therefore:

$$\begin{Bmatrix} F_{xH} \\ F_{yH} \\ F_{zH} \end{Bmatrix} = \left[T_{HB}\right] \begin{Bmatrix} F_{xB} \\ F_{yB} \\ F_{zB} \end{Bmatrix} \tag{39a}$$

and

$$\begin{Bmatrix} M_{xH} \\ M_{yH} \\ M_{zH} \end{Bmatrix} = \left[T_{HB}\right] \begin{Bmatrix} M_{xB} \\ M_{yB} \\ M_{zB} \end{Bmatrix} + e \begin{Bmatrix} 0 \\ -F_{zH} \\ F_{yH} \end{Bmatrix} \tag{39b}$$

Such loads due to all blades are then assembled to give the resultant forces and moments in the non-rotating system $F_{xHN}, F_{yHN}, F_{zHN}$, $M_{xHN}, M_{yHN}, M_{zHN}$. A generic scheme for the case of identical blades behavior may be found in Ref. 21.

Trim

To assure a trimmed steady flight, the present solution procedure is supplemented by seven equations which enables the introduction of seven unknown trim parameters. These unknowns are the fuselage attitude angles θ_{Fx} and θ_{Fy} ($\theta_{Fz}=0$ is assumed), the collective pitch angle θ_0, the cyclic pitch angles θ_{1c} and θ_{1s}, the tail rotor thrust T_R, and the averaged induced velocity $\bar{v}_i$. The corresponding equations are based on forces and moments of equilibrium in the F system and on Glauert's classical momentum equation for the averaged inflow:

$$F_{xHN} + F_{wx} - 1/2\ \rho_a V^2 S_x C_D = 0 \tag{40a}$$

$$F_{yHN} + F_{wy} + T_R - 1/2\ \rho_a V^2 S_y C_D = 0 \tag{40b}$$

$$F_{zHN} + F_{wz} - 1/2\ \rho_a (V_z + F_v \bar{v}_{io})^2 S_z C_D = 0 \tag{40c}$$

$$M_{xHN} + y_h F_{zHN} - z_h F_{yHN} + y_{cg} F_{wz} - z_{cg} F_{wy} +$$

$$+ y_{cp} F_{Az} - z_{cp} F_{Ay} - z_T T_R = 0 \tag{40d}$$

$$M_{yHN} + z_h F_{xHN} - x_h F_{zHN} + z_{cg} F_{wx} - x_{cg} F_{wz} +$$

$$+ z_{cp} F_{Ax} - x_{cp} F_{Az} + Q_{TR} = 0 \tag{40e}$$

$$M_{zHN} + x_h F_{yHN} - y_h F_{xHN} + x_{cg} F_{wy} - y_{cg} F_{wx} +$$

$$+ x_{cp} F_{Ay} - y_{cp} F_{Ax} + x_T T_R = 0 \tag{40f}$$

$$C_T/2\sqrt{\mu^2+\lambda^2} - \lambda_i = 0 \qquad (40g)$$

In these equations, V_x, V_y, V_z are the helicopter flight velocity components in the F (fuselage) system obtained by the U,V,W velocity components which were defined in the G systems. S_x, S_y, S_z are the fuselage flat-plate areas in the fuselage system directions and C_D is the corresponding drag coefficient. $F_v(\mu)$ is an empirical function of the advanced ratio, $\mu(\cong V_x/\Omega R)$, and accounts for the fuselage download due to the rotor inflow. F_{wx}, F_{wy}, F_{wz} are the fuselage weight components in the fuselage system coordinates, x_{cg}, y_{cg}, z_{cg} and x_{cp}, y_{cp}, z_{cp} are the center of gravity and center of pressure coordinates, respectively (measured from an arbitrary reference location). x_h, y_h, z_h and x_T, z_T are the rotor hub and tail rotor coordinates, respectively. C_T is the rotor thrust coefficient while $\lambda_i = \bar{v}_i/\Omega R$ and $\lambda \cong (V_z + \bar{v}_i)/\Omega R$.

Method of Solution

As already indicated, the present method of solution is based on the combination of the Harmonic Variables technique with generic algorithms for solving nonlinear systems. To demonstrate this combination, the following generic nonlinear system is considered

$$r_i(x_1, x_2 \ldots x_n) = 0 \qquad (i=1,n) \qquad (41)$$

where $\{x_i\}=\langle x_1, x_2 \ldots x_n \rangle^T$ is the vector of independent unknowns and $\{r_i\}=\langle r_1, r_2 \ldots r_n \rangle^T$ is the residuals vector which may generally be expressed using nonlinear operators. A general purpose nonlinear solver which was designed for determining the vector $\{x_i\}$ that will satisfy Eqs. (41), is usually based on two main components. The first component is "the algorithm" which includes the logic of the nonlinear solution (such as the Newton-Raphson method, quasi-linearized iterations etc.). Starting from an initial guess, $\{x_i^0\}$, this component reaches the desired solution by successive substitutions of trial vectors, $\{x_i^t\}$, in the second component that may be titled "the equations". This component evaluates the equations residuals $\{r_i^t\}$ for each trial vector. Depending on the solution algorithm, the trial vectors are selected in a way that the solution vector $\{x_i^s\}$ may be deduced.

In the present formulation, all time-dependent variables are defined as harmonic variables and therefore, by putting all the governing equations in an homogeneous form and using the mathematical operations between harmonic variables, the equation residuals are also obtained as harmonic variables. Therefore, in the present analysis, the $\{x_i\}$ vector contains the harmonic coefficients of all unknown harmonic variables and the residual vector, $\{r_i\}$, contains the harmonic coefficients of all the residuals harmonic variables. Thus, for n time-dependent unknowns, n·q scalar unknowns are produced (see Eq. (2) for the definition of q). In addition, scalar unknowns may be added to the above residual vector.

It should be emphasized again, that since operations between harmonic variables are executed automatically (see for example the multiplication operation in Fig. 1), both analytic and coding efforts are reduced to the expression of the governing equations in their homogeneous form, while no additional adaptation or discretization is needed.

RESULTS

The capability of the present formulation and method of solution to determine the rotor-fuselage nonlinear coupled response will be presented through the exploration of the effectiveness of conventional higher harmonic pitch inputs and the fuselage influence. For demonstration purposes, only the collective higher harmonic pitch control will be presented and discussed. The following results are for typical full scale hingeless four bladed rotor in forward flight (μ=0.3).

Case a: Isolated Rotor Response

In this case, the fuselage is assumed to be infinitely stiff and massive enough so that the hub motions may be neglected.

Generally, the higher harmonic control pitch command is expressed for four bladed rotor as:

$$\theta_{H(k)} = A_{col}\cos(4\psi_1 - \varphi_{col}) + A_{lat}\cos(4\psi_1 - \varphi_{lat})\cos\psi_k + A_{long}\cos(4\psi_1 - \varphi_{long})\sin\psi_k \qquad (42)$$

ψ_k is the azimuth angle of the $k^{\underline{th}}$ blade while the first blade is the reference one ($\psi=\psi_1$). $\theta_{H(k)}$ presents the higher harmonic control that is superimposed on the $\theta_o+\theta_{1c}\cos\psi_k+\theta_{1s}\sin\psi_k$ pitch command which is determined by trim considerations (see Eqs. 40a-g).

First, the influence of higher harmonic collective pitch is presented. The 4/rev. amplitude of the three hub shear components F_x, F_y, F_z and two of the moment components M_x, M_y are presented in Figs. 5a-c as function of φ_{col} for A_{col}=0.005 rad, and compared with the base line value (the M_z vibratory component is assumed to be absorbed by the engine). As shown, the most effective phase angle is different in each direction and the most influenced component is F_z, where the 4/rev. vibratory amplitude may be reduced from 596 Nt to 95 Nt by $\varphi_{col} \cong 126^\circ$.

To study the dependency of this behavior on the higher harmonic control amplitude, Figs. 6a-c present the amplitude changes due to collective higher harmonic control as function of the A_{col} value. As shown, in most cases linear variations are observed. This indicates that the higher harmonic effectiveness is constant. However, in the most important component, F_z, the beneficial lower branch (of $\varphi_{col}=120^\circ$) exhibits nonlinear behavior by having a minimum value around A_{col}=0.0055.

For better insight into the mechanism associated with the vibratory amplitude changes presented in Figs. 5, 6, the effective angle of attack is shown in Fig. 7 for A_{col}=0.005 $\varphi_{col}=120^\circ$. In terms of the

present formulation, this angle is determined by (see Eqs. 32,33):

$$\alpha(\psi) = tg^{-1}\left(\frac{Q(\psi)}{U_B(\psi)}\right) \qquad (43)$$

As shown, the changes in the effective angle of attack are of 4/rev. nature and are relatively small. Note that these variations are not the direct outcome of the higher harmonic pitch control since the determination of the effective angle of attack includes also the influence of the resulting dynamic response. Further, the resulting root vertical hub shear in the rotating frame with and without the higher harmonic pitch command is presented in Fig. 8. Although, the variations are of

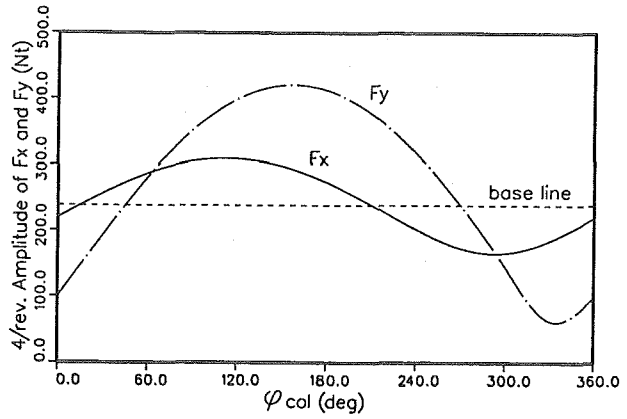

Fig. 5a: The influence of higher harmonic collective pitch on F_x and F_y as function of φ_{col} (A_{col}=0.005 rad).

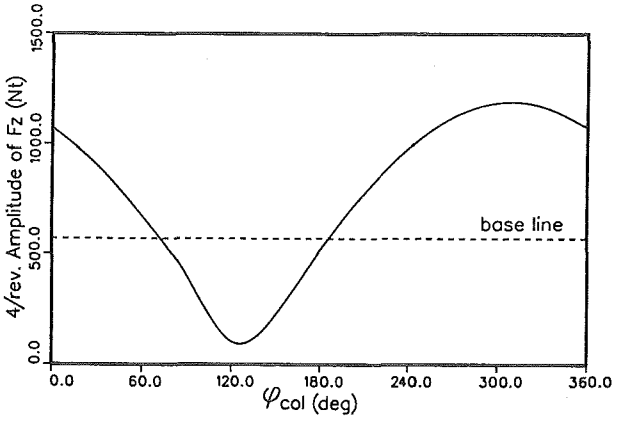

Fig. 5b: The influence of higher harmonic collective pitch on F_z as function of φ_{col} (A_{col}=0.005 rad).

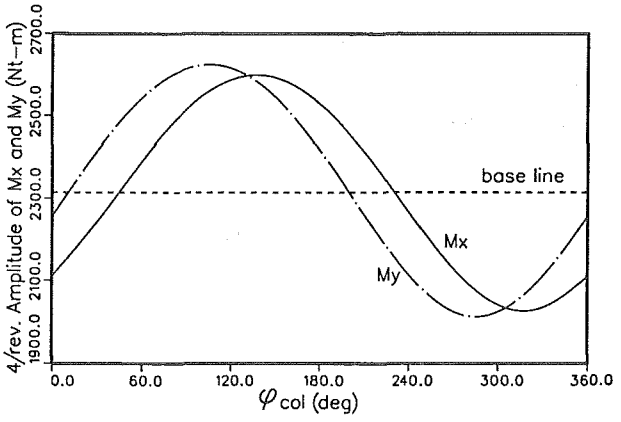

Fig. 5c: The influence of higher harmonic collective pitch on M_x and M_y as function of φ_{col} (A_{col}=0.005 rad).

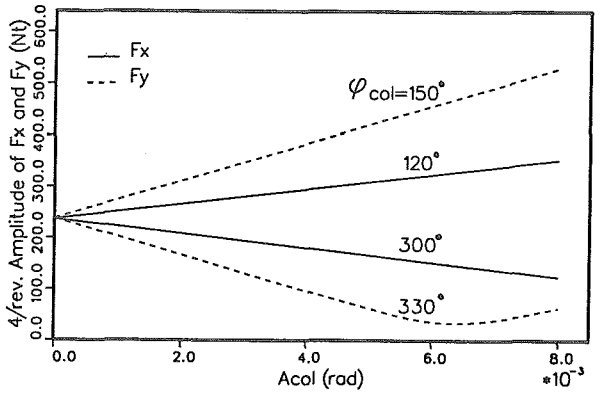

Fig. 6a: The influence of higher harmonic collective pitch on F_x and F_y as function of A_{col}.

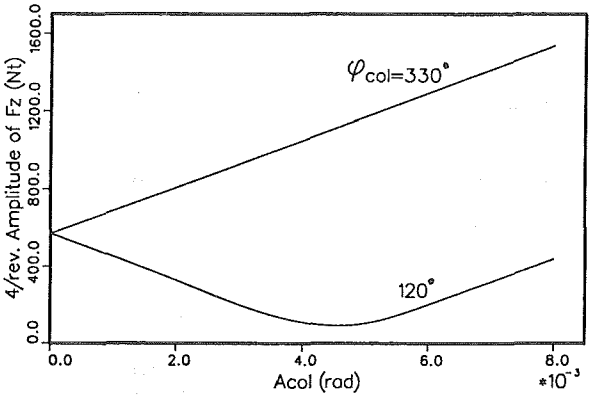

Fig. 6b: The influence of higher harmonic collective pitch on F_z as function of A_{col}.

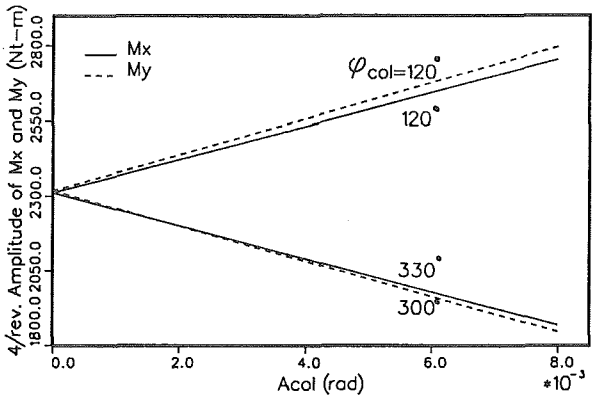

Fig. 6c: The influence of higher harmonic collective pitch on M_x and M_y as function of A_{col}.

4/rev. nature, the structural dynamic effects induce a phase shift between this behavior and that of the effective angle of attack (see Fig. 7) Assembling all blades contributions to the non-rotating frame shows a pure 4/rev. vibratory force where the effectiveness of the higher harmonic control is evident (see Fig. 9).

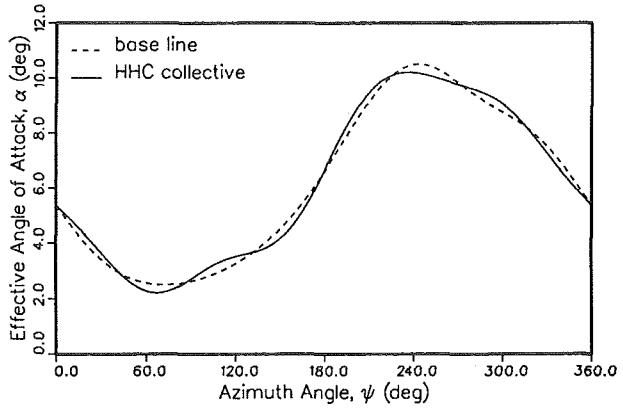

Fig. 7: The effective angle of attack with and without higher harmonic collective pitch (A_{col}=0.005 rad, φ_{col}=120°).

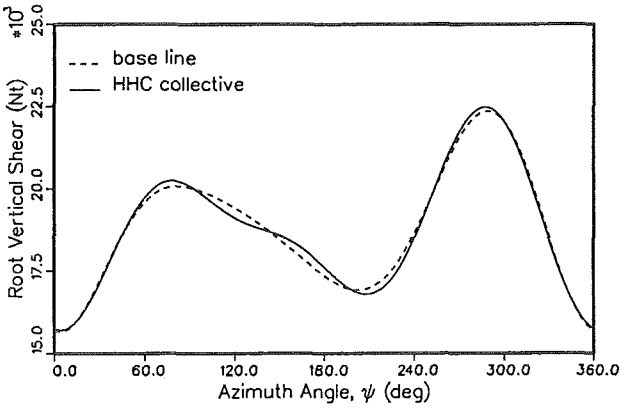

Fig. 8: The root vertical hub shear in the rotating frame with and without higher harmonic collective pitch (A_{col}=0.005 rad, φ_{col}=120°).

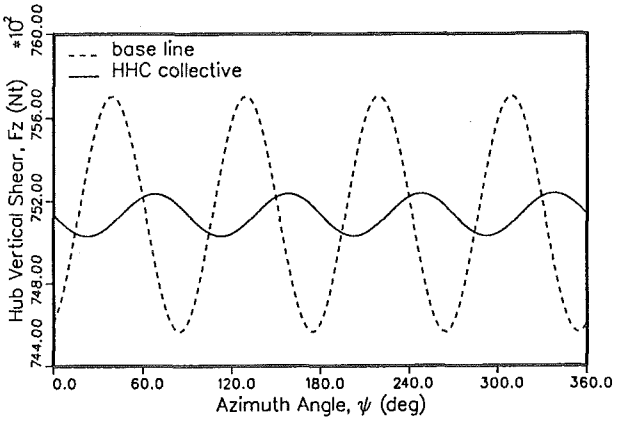

Fig. 9: The hub vertical shear in the non-rotating frame with and without higher harmonic collective pitch (A_{col}=0.005 rad, φ_{col}=120°).

Case b: Coupled Rotor-Fuselage Response

To investigate a vast range of fuselage properties, the fuselage response at the hub has been characterized by its magnitude, R (measured in g/Nt) and the phase lag of its response, β. Figure 10a presents the 4/rev. amplitude of the vertical force, F_z, which is transferred to the fuselage as function of R for different values of β. The values of the fuselage response which may be obtained in realistic fuselages are also indicated while the corresponding values of the phase lag depend on the damping in the fuselage structure. Figure 10b presents the hub acceleration amplitude for each curve of Fig. 10a. The symbols in Figs. 10a represent constant acceleration amplitudes.

As shown, for very stiff and massive fuselage (large values of R), the 4/rev. amplitude of F_z coincides with the base line which has been discussed above in the case of isolated rotor, while the hub acceleration amplitude vanishes. As the fuselage became elastic and less massive, the hub acceleration amplitude raises. However, it is possible to adjust the fuselage structural damping (which reflects itself by the phase angle, β) so that for a given value of R, both hub acceleration amplitude and the vibratory force amplitude will be

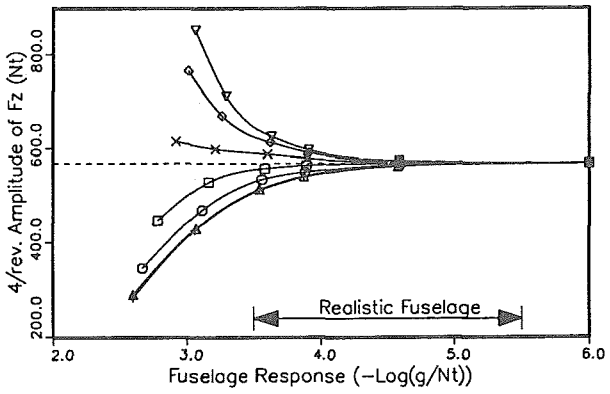

Fig. 10a: The fuselage influence on F_z as function of its response magnitude and phase.

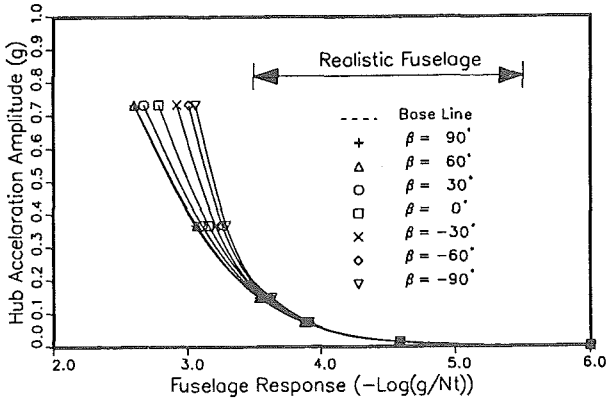

Fig. 10b: The fuselage influence on hub acceleration as function of its response magnitude and phase.

minimal. Note that Figs. 10a,b covers all possible linear fuselages characterized by their response at the hub. However, it is expected that the acceleration amplitude at any other point of interest on the fuselage (such as the pilot seat) will be only slightly different.

CONCLUDING REMARKS

A theoretical modeling of rotor/fuselage coupled response has been presented. The model is based on advanced frequency domain computational techniques that enable the incorporation of high harmonics in nonlinear formulation. The model may be used for predicting the fully unsteady coupled response due to harmonic pitch commands and may serve as the analysis component in a comprehensive optimization scheme. The effects of collective higher harmonic pitch control and elastic fuselage were demonstrated and discussed. It has been shown that the effectiveness of collective higher harmonic pitch control is not always constant and is changed significantly as function of its magnitude and phase angle. It has been also shown that adjusting fuselage damping may reduce both hub acceleration magnitude and vibratory vertical hub force.

References

1. Johnson, W., "Self-Tuning Regulators for Multicycle Control of Helicopter Vibrations", NASA Technical Paper 1996, 1982.
2. Friedmann, P.P., "Helicopter Rotor Dynamics and Aeroelasticity: Some Key Ideas and Insights", Vertica, Vol. 14, No. 1, pp. 101-121, 1990.
3. Wood, R.E., Powers, R.W., Cline, J.H. and Hammond, C.E., "On Developing and Flight Testing a Higher Harmonic Control System", J. Am. Helicopter Soc., Vol. 30, No. 1, pp. 3-20, Jan. 1985.
4. Miao, W. and Frye, H.M., "Flight Demonstration of Higher Harmonic Control (HHC) on S-76", 42nd Annual Forum of the AHS, Washington, D.C., June 1986.
5. Polychroniadis, M. and Achache, M., "Higher Harmonic Control: Flight Tests of an Experimental System on SA 349 Research Gazelle", 42nd Annual Forum on the AHS, Washington, DC, June 1986.
6. Shaw, J., Albion, N., Hanker, E.J. and Teal, R.S., "Higher Harmonic Control: Wind Tunnel Demonstration of Fully Effective Vibratory Hub Force Suppression", J. Am. Helicopter Soc., Vol. 34, No. 1, pp. 14-25, Jan. 1989.
7. Lehmann, G., "The Effect of Higher Harmonic Control (HHC) on a Four-Bladed Hingeless Model Rotor", Vertica, Vol. 9, No. 3, pp. 273-284, 1985.
8. Taylor, R.B., Farrar, F.A. and Miao, W., "An Active Control System for Helicopter Vibration Reduction by Higher Harmonic Pitch", AIAA Paper No. 80-0672, 36th Annual Forum, AHS, Washington, D.C., May 1980.
9. Molusis, J.A., "The Importance of Nonlinearity on the Higher Harmonic Control of Helicopter Vibration", 39th Annual Forum of the AHS, St. Louis, MO, May 1983.
10. Chopra, I. and J.L. McCloud, "A Numerical Simulation Study of Open-Loop, Closed-Loop and Adaptive Multicyclic Control Systems", J. Am. Helicopter Soc., Vol. 28, No. 1, January 1983.
11. Robinson, L.H. and Friedmann, P.P., "Analytic Simulation of Higher Harmonic Control Using a New Aeroelastic Model", AIAA Paper Paper 89-1321-CP, Proc. AIAA/ASME/ASCE/AHS 30th Structures, Structural Dynamics and Materials Conference, Mobile, AL, Part III, pp. 1394-1406, April 1989.
12. Nguyen, K. and Chopra, I., "Application of Higher Harmonic Control (HHC) to Hingeless Rotor Systems", AIAA Paper No. 89-1215-CP, Proc. AIAA/ASME/ASCE/ ACS 30th Structures, Structural Dynamics and Materials Conf., Mobile, AL, pp. 507-520, April 1989.
13. Papavassiliou, I., Venkatesan, C. and Friedmann, P.P., "A Study of Coupled Rotor-Fuselage Vibration with Higher Harmonic Control Using a Symbolic Computing Facility", Proc. of the 16th European Rotorcraft Forum, Glasgow, UK, pp. III.7.3.1-III.7.3.23, Sept. 18-21, 1990.
14. Ham, N.D., "Helicopter Individual-Blade-Control Research at MIT 1977-1985", Vertica, Vol. 11, pp. 109-122, 1986.
15. Ham, N.D., "Helicopter Individual-Blade-Control and Its Applications", 39th Annual Forum of the AHS, St. Louis, MO, May 1983.
16. Rand, O., "Harmonic Variables - A New Approach to Nonlinear Periodic Problems", Journal of Computers and Mathematics with Applications, Vol. 15, No. 11, pp. 953-961, 1988.
17. Rosen, A. and Rand, O., "Numerical Model of the Nonlinear Behavior of Curved Rods", Computers and Structures, Vol. 22, No. 5, pp. 785-799, 1986.
18. Dompka, R.V., et al., "Plan, Formulate, and Discuss a NASTRAN Finite-Element Model of the BELL-ACAP Helicopter Airframe", Summary Report 699-099-218, December 1986.
19. Greenberg, J.M., "Airfoil in Sinusoidal Motion in Pulsating Stream", NACA TN-1329, 1947.
20. Rand, O., "Influence of Interactional Aerodynamics on Rotor/Fuselage Coupled Response in Hover and Forward Flight", J. Am. Helicopter Soc., Vol. 34, No. 4, pp. 28-36, 1989.
21. Bramwell, A.R.S., *Helicopter Dynamics*, Edward Arnold (Publishers) Ltd., 1986.